Supplemental Material for
"Measurement of total phase fluctuation in cold-atomic quantum simulators"

Taufiq Murtadho,[1,*] Federica Cataldini,[2] Sebastian Erne,[2] Marek Gluza,[1]
Mohammadamin Tajik,[2] Jörg Schmiedmayer,[2] and Nelly H.Y. Ng[1,†]

[1] *School of Physical and Mathematical Sciences, Nanyang Technological University, 639673 Singapore*
[2] *Vienna Center for Quantum Science and Technology, Atominstitut, TU Wien, Stadionallee 2, 1020 Vienna, Austria*

CONTENTS

I. BOGOLIUBOV SAMPLING FOR IN SITU FLUCTUATIONS AND THERMOMETRY

This section states the formula for sampling thermal in situ fluctuations of uniform decoupled 1D gases from Bogoliubov modes, including Eq. (5) in the main text. We also derive the expression connecting the coherence length to temperature used for thermometry in the main text. This section is a restatement of various results in the literature, e.g. Refs. [1, 2].

We start from the standard Bogoliubov modes expansion

$$\hat{\phi}_{\pm}(z,t) = \frac{1}{\sqrt{2n_{\mathrm{1D}}}} \sum_{k\neq 0} f_{\phi,k}(z) e^{-i\varepsilon_k t/\hbar} \hat{b}_k + \mathrm{h.c.} \tag{S-1}$$

$$\delta\hat{n}_{\pm}(z,t) = \sqrt{2n_{\mathrm{1D}}} \sum_{k\neq 0} i f_{n,k}(z) e^{-i\varepsilon_k t/\hbar} \hat{b}_k + \mathrm{h.c.}, \tag{S-2}$$

where n_{1D} is the mean density of a *single* condensate ($n_{\mathrm{1D}} = n_0/2$). The summation is taken over both positive and negative wave vectors k. The eigenfunctions $f_k^{\pm}(z)$ and eigenenergies ε_k are given by

$$\varepsilon_k = \sqrt{E_k(E_k + 2gn_{\mathrm{1D}})} \tag{S-3}$$

$$f_{\phi,k}(z) = \sqrt{\frac{\varepsilon_k}{E_k}} \frac{1}{\sqrt{L}} e^{ikz} \qquad f_{n,k}(z) = \sqrt{\frac{E_k}{\varepsilon_k}} \frac{1}{\sqrt{L}} e^{ikz}, \tag{S-4}$$

with $E_k = (\hbar k)^2/2m$ being the free particle spectrum. The occupations $\hat{b}_k$ are sampled from a complex normal distribution whose variance is given by the mean occupation of Bose-Einstein distribution, i.e.

$$b_k = \sqrt{\frac{\eta_k^{\pm}}{2}} (u_k + i u_k') \qquad \eta_k^{\pm} = \frac{1}{\exp(\frac{\varepsilon_k}{k_B T_{\pm}}) - 1}, \tag{S-5}$$

where u_k, u_k' are random real numbers independently sampled from a normal distribution, and $T_{\pm}$ being the temperatures of the symmetric and antisymmetric fields respectively.

* fiqmurtadho@gmail.com
† nelly.ng@ntu.edu.sg

The vertex correlation function for the total phase is written as

$$C_+(z) = \langle \cos[\phi_+(z) - \phi_+(0)] \rangle = \exp\left(-\frac{1}{2} \left\langle [\phi_+(z) - \phi_+(0)]^2 \right\rangle \right), \tag{S-6}$$

with the variance of the phase given by

$$\left\langle [\phi_+(z) - \phi_+(0)]^2 \right\rangle = \frac{1}{n_{1\mathrm{D}} L} \sum_{k \neq 0} \frac{\varepsilon_k}{E_k} (1 + 2\overline{n}_k^+) \, (1 - \cos(kz)) \, . \tag{S-7}$$

In the thermodynamic limit of $L \to \infty$ the summation over discrete modes can be replaced with integral. After using Rayleigh-Jeans approximation $\overline{n}_k^+ \approx k_B T_+ / \varepsilon_k$ and ignoring the quantum fluctuation terms, one finds

$$\lim_{L \to \infty} \left\langle [\phi_+(z) - \phi_+(0)]^2 \right\rangle \approx 2 \frac{|z|}{\lambda_{T_+}} \qquad \lambda_{T_+} = \frac{\hbar^2 n_{1\mathrm{D}}}{m k_B T_+}. \tag{S-8}$$

Thus, in $L \to \infty$ limit, $C_+(z)$ decays exponentially with length scale λ_{T_+}. However, for systems with finite L, the correlation function is generally expressed in terms of a summation over a finite number of modes. Therefore, the temperature fitted with an exponential decay model could underestimate the true temperature.

II. EXTENDED NUMERICAL DATA

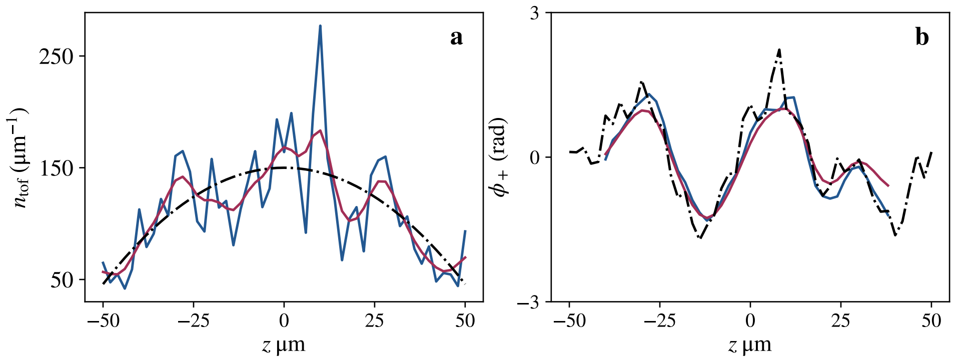

FIG. S1. *The effect of mean density curvature and finite imaging resolution*.- In the main text, the numerical benchmarking is implemented in a homogeneous gas for simplicity. However, our extraction method is also applicable for sufficiently smooth mean densities such as that of a harmonic trap. In panel (**a**), we show density ripples (solid blue) generated by fluctuations with inverse parabolic mean density (black dashed line). The effect of finite imaging resolution in experiments is simulated by setting the pixel size to be that of vertical imaging (2 μm) and convolving the density ripple with a Gaussian filter of width $\sigma = 3$ μm (solid red) [3]. In panel (**b**), we show that the extracted total phase is not significantly influenced by convolution. The red (blue) solid line is the extracted total phase from density ripples with (without) convolution and the black dashed line is the input profile. The expansion time is $\tau = 16$ ms.

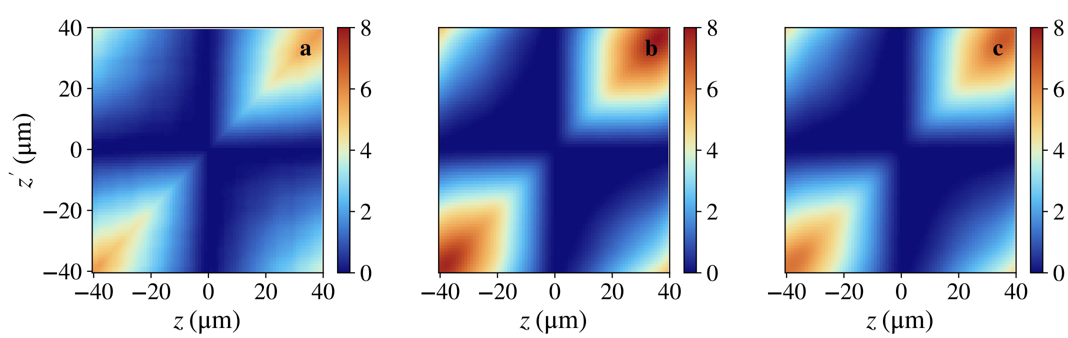

FIG. S2. *Reconstruction of the two-point correlation function* $G(z, z')$.- (**a**) Input $G(z, z')$ computed with 10^3 thermal samples having temperature $T_+ = 50$ nK. This panel is identical to Fig. 2c in the main text. Panels (**b**) and (**c**) show TOF reconstruction with (**b**) $\tau = 11$ ms and (**c**) $\tau = 16$ ms. Panel (**c**) is identical to Fig. 2d in the main text.

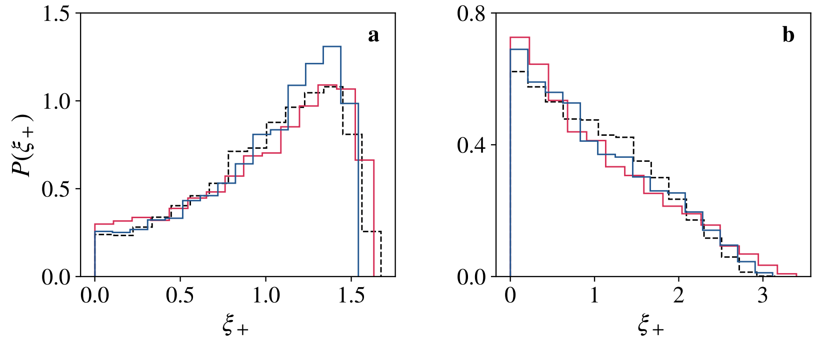

FIG. S4. *The reconstruction of full contrast distribution function.*– In this plot, we show the reconstruction the full contrast distribution function $P(\xi_+)$ where $\xi_+(l) = |C_+(l)|^2/\langle|C_+(l)|^2\rangle$ and $C_+(l) = \int_{-l/2}^{l/2} e^{i\phi_+(z)} dz$ with $0 < l \leq L$. The corresponding distribution for the relative phase $P(\xi_-)$ has been used to characterize quantum and thermal noise in Luttinger liquid [2, 4] as well as to study prethermalization after coherent splitting [5]. The red (blue) histogram shows the estimated distribution from our extraction with $\tau = 11$ ms ($\tau = 16$ ms), while the black (dashed-dotted) histogram displays the distribution computed with the input samples. Each distribution is computed with 10^4 samples with (**a**) $l = 20$ μm and (**b**) $l = 60$ μm for a total length of $L = 100$ μm. From this plot, it is clear that our extraction method can faithfully reconstruct the full contrast distribution function $P(\xi_+)$.

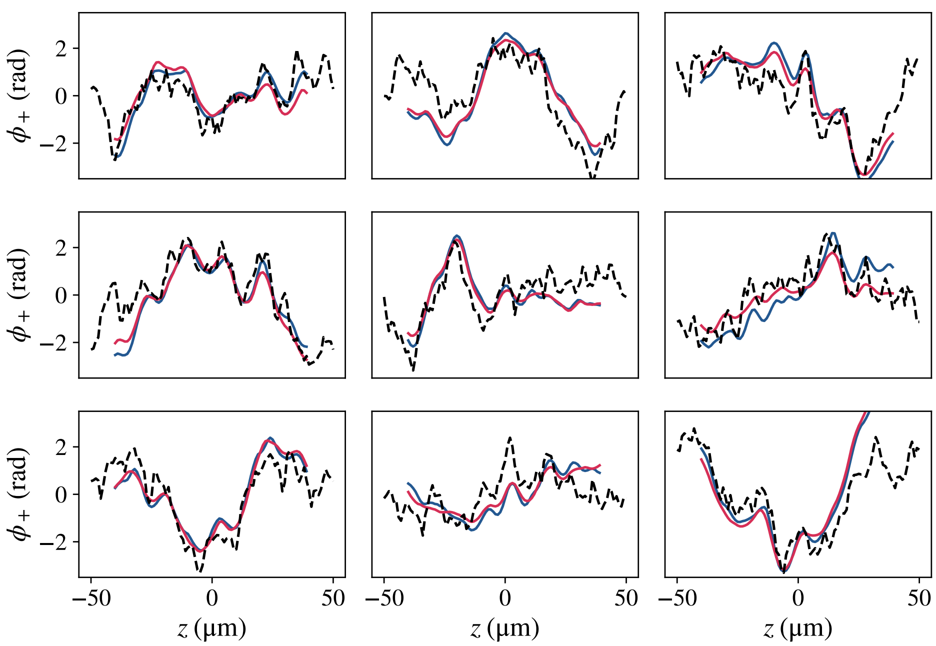

FIG. S3. *Single shots examples*.- A few single shots examples of total phase extraction with uniform mean density and input phases (black dashed lines) sampled with the Bogoliubov sampling method (see Sec. I). The blue (red) solid line corresponds to reconstructed profiles after $\tau = 11$ ms ($\tau = 16$ ms) time of flight (TOF). The parameters are the same as in Fig. 1 and Fig. 2 in the main text.

III. EXPERIMENTAL DETAILS AND PROTOCOLS

A. Experiment 1: Relaxation of driven Luttinger liquids

In our AtomChip setup, laser-cooled ^{87}Rb atoms are cooled deep into quantum degeneracy and loaded into a double-well (DW) of two parallel cigar-shaped harmonic wells realized by radio-frequency (RF) dressed-state potentials. The tight transverse confinement ($\omega_\perp \approx 2\pi \times 1.4$ kHz) and weak longitudinal confinement ($\omega_z \approx 2\pi \times 7$ Hz) realize two parallel 1D quasicondensates. During the experiment, we keep the DW to be symmetric and with a high barrier to ensure the two clouds are decoupled.

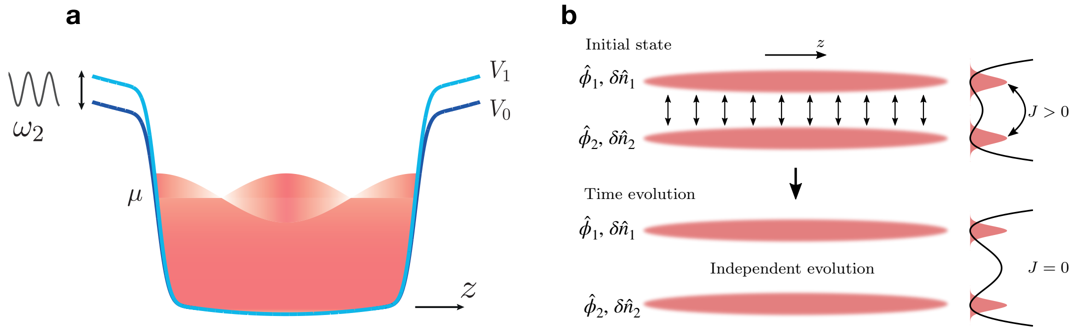

FIG. S5. *Schematics of the experimental examples.*- (**a**) Schematic of driven Luttinger liquid experiment (Experiment 1). The system is prepared at $t = -t_0$ in a thermal state of the box-like potential V_0 having length L. For $t_0 \leq t \leq 0$, the potential height is continuously modulated at a driving frequency $\omega_2 = c(2\pi/L)$ (c is the speed of sound) between V_0 and V_1. The atoms are regularly pushed from the edges towards the center of the trap hence inducing an oscillation of the chemical potential μ. For $t > 0$, the driving is permanently turned off, and the gas evolves in the potential V_0. (**b**) Schematic of the quench experiment (Experiment 2), adapted from Ref. [6]. A pair of parallel 1D quasicondensates are trapped in a double-well (DW) and allowed to tunnel with tunnelling rate $J > 0$. The system is let to reach thermal equilibrium before undergoing a quench $J \to 0$ implemented by ramping up the DW barrier. The time evolution of the system is then probed by extracting $\phi_\pm(z) = \hat{\phi}_1(z) \pm \hat{\phi}_2(z)$ from interference pictures measured by vertically imaging the atoms after 15.6 ms TOF.

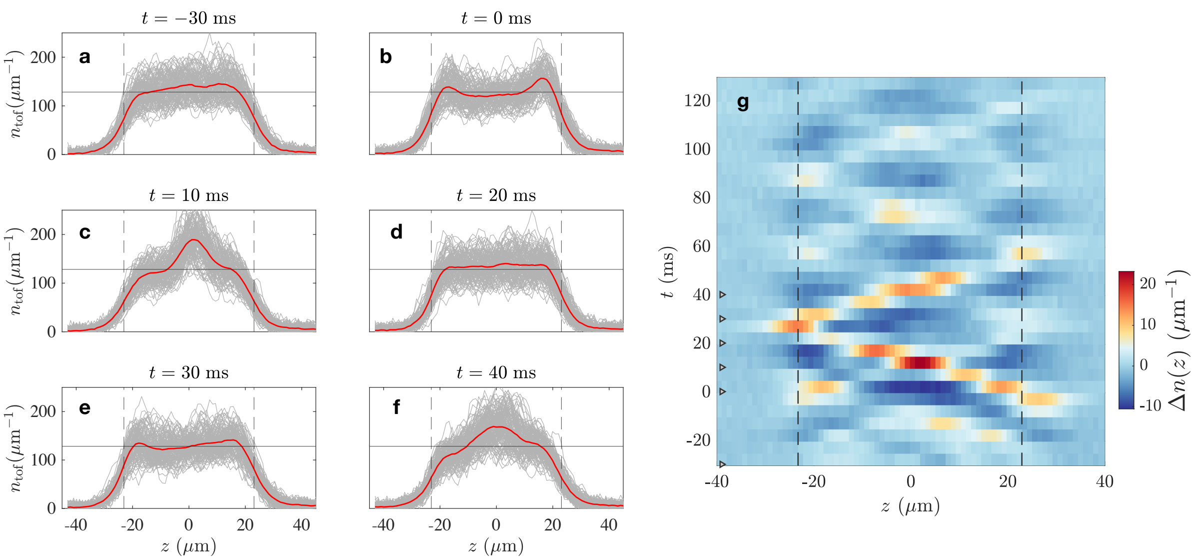

FIG. S6. *Density ripples data from driven Luttinger liquids experiment*.- Out of equilibrium dynamics after driving is probed every $\Delta t = 5$ ms time step by measuring density ripples $n_{\rm tof}(z)$ after $\tau = 11.2$ ms TOF measurement. Experimental repetition for each time step is ~ 130 shots. Panels (**a**) - (**f**) show a single realization (grey) and average signal (red) of density ripples at different evolution times. Negative times refer to the driving period, while positive times represent the subsequent evolution. In particular, panel (**a**) is for $t = -30$ ms when the system is in thermal equilibrium, before the driving protocol is on. The black solid line indicates mean linear density $n_0 \approx 128(10)$ $\mu{\rm m}^{-1}$ calculated in thermal equilibrium. We drive the system with frequency resonant to the second mode $\omega_2 = 2\pi \times 36$ Hz $\approx k_2 c$ with $k_2 = 2\pi/L$ ($L \approx 46(3)$ μm, see dashed lines) and $c \approx 1.8$ μm/s being the speed of sound for each well. The driving is stopped at $t = 0$ ms with density ripples shown in panel (**b**) and the system is subsequently let to evolve naturally. In extracting $\phi_+(z)$, we also take into account slight spatial curvature in mean density $n_0(z)$ due to overlap between magnetic and dipole potential. Panel (**g**) displays the evolution of the mean density perturbation $\Delta n(z,t) = \langle n_{\rm tof}(z,t)\rangle - \overline{\langle n_{\rm tof}(z,t)\rangle}$ where overline denotes average over time. For long enough evolution times, $\overline{\langle n_{\rm tof}(z,t)\rangle}$ is equal to $n_0(z)$ up to a loss in atomic number. During the 130 ms of evolution, heating of the system is negligible and the measured atom loss rate is about 1 atom/ms, with the total atom number being about 3400. The measured loss arises from three-body recombination, collisions with the background gas particles and technical noise. The small triangles on the side represent some selected time step for which the full density profile $n_{\rm tof}(z)$ is shown in panels (**a**) - (**f**).

The potential in the longitudinal direction is shaped into a box-like trap by shining a blue-detuned laser light ($\lambda = 767$ nm) from the transverse direction [7]. By inserting a mask aligned such that it shields the center of the atomic clouds from the light beam, two steep walls form on the sides of the atoms. We then modulate the amplitude of the dipole laser at a frequency resonant to the second phononic mode $\omega_2 = c\, k_2 = c\, 2\pi/L \approx 36$ Hz (see Fig. S5a), creating excitations in the system . The modulation lasts for 30 ms, corresponding to approximately one period, after which the system is let to evolve for 130 ms. The excitation at time t is probed by extracting the density profiles $n_{\rm tof}(z,t)$ from absorption pictures taken after 11.2 ms of time of flight (TOF) with the imaging beam sent from the transverse direction. We repeat the experimental procedure approximately 130 times at each evolution time t to collect a statistically large set of data.

The result from total phase thermometry of the initial state (before driving) is benchmarked with density ripple thermometry [8–10], whereby the density-density correlation function

$$g_1(\Delta z) = \frac{\langle n_{\rm tof}(z) n_{\rm tof}(z+\Delta z)\rangle}{\langle n_{\rm tof}(z)\rangle \, \langle n_{\rm tof}(z+\Delta z)\rangle} \tag{S-9}$$

is computed from experimental data. By comparing theory and experiment, thermal coherence length $\lambda_{T_+} = 12(2)\ \mu\mathrm{m}$ corresponding to a temperature $T_+ = 30(5)$ nK is fitted, in excellent agreement with our result. The extended experimental data for the relaxation after driving is given in Fig. S6

B. Experiment 2: Dynamics of total phase after quench

The setup for the second example is the one from the Gaussification experiment [6]. It is similar to above (Experiment 1) but without the dipole laser light and the mask. Moreover, the DW barrier is initially lowered such that the two 1D quasicondensates are coupled through tunnelling (see Fig. S5b). Detailed experimental protocols can be found in Ref. [6].

The low-energy Hamiltonian of two tunnel-coupled parallel 1D superfluids is given by [11]

$$H = H_{SG}^{(-)} + H_{LL}^{(+)} \tag{S-10}$$

with the relative sector being described by the sine-Gordon model [11, 12]

$$H_{SG}^{(-)} = \int dz \left[\frac{\hbar^2 n_0}{4m}(\partial_z\phi_-)^2 + \frac{g}{4}(\delta n_-)^2 - 2\hbar J n_0 \cos\phi_-\right], \tag{S-11}$$

while the total sector is described by Luttinger liquid

$$H_{LL}^{(+)} = \int dz \left[\frac{\hbar^2 n_0}{4m}(\partial_z\phi_+)^2 + \frac{g}{4}(\delta n_+)^2\right]. \tag{S-12}$$

The system is initially prepared in thermal equilibrium of H with $J > 0$. Then, it is pushed out of equilibrium by quenching to decoupled gases $J \to 0$ implemented through the raising of DW barrier within $2\ \mathrm{ms}$. Since the system is initialized in thermal equilibrium and the quench only affects the relative sector, the total sector is expected to stay in thermal equilibrium with approximately constant temperature.

The Hamiltonian (S-10) omits the coupling term between the relative and total sector, which can be justified in equilibrium or near equilibrium. Meanwhile, the two sectors are expected to be coupled in general out-of-equilibrium scenarios [11–13]. The analysis presented in this work will allow us to study this intersector coupling in future experiments.

---

[1] T. Giamarchi, *Quantum Physics in One Dimension*, Vol. 121 (Clarendon Press, Oxford, 2003).

[2] H.-P. Stimming, N. J. Mauser, J. Schmiedmayer, and I. E. Mazets, Fluctuations and stochastic processes in one-dimensional many-body quantum systems, Phys. Rev. Lett. **105**, 015301 (2010).

[3] T. Murtadho, M. Gluza, K. Z. Arifa, S. Erne, J. Schmiedmayer, and N. H. Y. Ng, Systematic analysis of relative phase extraction in one-dimensional Bose gases interferometry, SciPost Phys. **18**, 065 (2025).

[4] S. Hofferberth, I. Lesanovsky, T. Schumm, A. Imambekov, V. Gritsev, E. Demler, and J. Schmiedmayer, Probing quantum and thermal noise in an interacting many-body system, Nat. Phys. **4**, 489 (2008).

[5] M. Gring, M. Kuhnert, T. Langen, T. Kitagawa, B. Rauer, M. Schreitl, I. Mazets, D. A. Smith, E. Demler, and J. Schmiedmayer, Relaxation and prethermalization in an isolated quantum system, Science **337**, 1318 (2012).

[6] T. Schweigler, M. Gluza, M. Tajik, S. Sotiriadis, F. Cataldini, S.-C. Ji, F. S. Møller, J. Sabino, B. Rauer, J. Eisert, *et al.*, Decay and recurrence of non-Gaussian correlations in a quantum many-body system, Nat. Phys. **17**, 559 (2021).

[7] B. Rauer, S. Erne, T. Schweigler, F. Cataldini, M. Tajik, and J. Schmiedmayer, Recurrences in an isolated quantum many-body system, Science **360**, 307 (2018).

[8] A. Imambekov, I. E. Mazets, D. S. Petrov, V. Gritsev, S. Manz, S. Hofferberth, T. Schumm, E. Demler, and J. Schmiedmayer, Density ripples in expanding low-dimensional gases as a probe of correlations, Phys. Rev. A **80**, 033604 (2009).

[9] S. Manz, R. Bücker, T. Betz, C. Koller, S. Hofferberth, I. E. Mazets, A. Imambekov, E. Demler, A. Perrin, J. Schmiedmayer, and T. Schumm, Two-point density correlations of quasicondensates in free expansion, Phys. Rev. A **81**, 031610 (2010).

[10] F. Møller, T. Schweigler, M. Tajik, J. a. Sabino, F. Cataldini, S.-C. Ji, and J. Schmiedmayer, Thermometry of one-dimensional Bose gases with neural networks, Phys. Rev. A **104**, 043305 (2021).

[11] V. Gritsev, A. Polkovnikov, and E. Demler, Linear response theory for a pair of coupled one-dimensional condensates of interacting atoms, Phys. Rev. B **75**, 174511 (2007).

[12] T. Schweigler, V. Kasper, S. Erne, I. Mazets, B. Rauer, F. Cataldini, T. Langen, T. Gasenzer, J. Berges, and J. Schmiedmayer, Experimental characterization of a quantum many-body system via higher-order correlations, Nature **545**, 323 (2017).

[13] J.-F. Mennemann, I. E. Mazets, M. Pigneur, H. P. Stimming, N. J. Mauser, J. Schmiedmayer, and S. Erne, Relaxation in an extended bosonic Josephson junction, Phys. Rev. Res. **3**, 023197 (2021).